DALTON

Multinuclear solid-state nuclear magnetic resonance studies on transition-metal clusters containing hydrides *

Taro Eguchi,[a] Brian T. Heaton,[b] Rachel Harding,[b] Kei Miyagi,[a] Giuliano Longoni,[c] Jens Nähring,[b] Nobuo Nakamura,[a] Hirokazu Nakayama,[a] Tapani A. Pakkanen,[d] Jouni Pursiainen[e] and Anthony K. Smith[b]

[a] *Department of Chemistry, Faculty of Science, Osaka University, Toyonaka, Osaka 560, Japan*
[b] *Department of Chemistry, University of Liverpool, Liverpool L69 3BX, UK*
[c] *Dipartimento di Chimica Fisica ed Inorganica, Viale del Risorgimento 4, 40136, Bologna, Italy*
[d] *Department of Chemistry, University of Joensuu, FIN-80101, Joensuu 10, Finland*
[e] *Department of Chemistry, University of Oulu, FIN-90570, Oulu, Finland*

Solid-state ^{1}H and D NMR measurements have been made for all transition-metal carbonyl clusters containing interstitial hydrides/deuterides previously characterised by neutron diffraction. There is a close agreement between the values of $\delta(^1H/D)$ in solution and the solid state except for $[Co_6H(CO)_{15}]^-$. The values of $\delta(^1H)$ for interstitial hydrides are in the range δ +18.5 to −26.8; the shift to high field is shown to be due to an increasing displacement of H from the centre of the metal octahedral cavity, consistent with surface tensor harmonic theory. Whereas migration of H readily occurs in both $[Rh_{13}H_x(CO)_{24}]^{(5-x)-}$ (x = 2 or 3) and $[Ru_2Rh_2H_2(CO)_{12}]$ in solution, solid-state ^{1}H NMR measurements on $[Rh_{13}H_x(CO)_{24}]^{(5-x)-}$ (x = 2 or 3) showed that there is no evidence for such migration in the solid state and for $[Ru_2Rh_2H_2(CO)_{12}]$ oscillation of H about the metal–metal edge(s) occurs rather than migration to different edges as found in solution.

There are now many examples of hydride transition-metal carbonyl clusters and the hydrogen site occupancy is difficult to predict. Examples of terminal, edge-, face-bridging and interstitial hydrides are known and unambiguous location comes only from neutron diffraction or solution NMR studies particularly when the metal has a nuclear spin, *e.g.* ^{103}Rh. Characterisation through multinuclear NMR measurements is particularly useful when the hydride clusters are only stable at low temperature preventing isolation of X-ray-quality crystals {*e.g.* terminal hydride $[Rh_6H(CO)_{15}]^-$,[1] edge-bridge hydride $[Rh_6HC(CO)_{13}]^-$,[2] face-bridge hydride $[Rh_6HC(CO)_{15}]^{-1}$} and for distinguishing between similar metals in heterometallic clusters *e.g.* $[Ru_2Rh_2H_2(CO)_{12}]$[3] (see below). However, hydrogen migration easily occurs in solution and, although solution NMR studies have been useful for elucidating the migratory mechanism(s), it is sometimes difficult to obtain static structures in solution because it is impossible to retain solubility at low temperatures and some migrations are of extremely low energy.

This paper reports solid-state NMR studies on: (1) all the transition-metal carbonyl clusters presently known to contain interstitial hydrides[4–6] in order better to understand the apparently wide variation of the hydride chemical shift in solution and the mobility of the hydride; (2) $[Rh_{13}H_x(CO)_{24}]^{(5-x)-}$ (x = 2 or 3) which previously has been found to undergo facile interstitial hydrogen migration;[7] and (3) $[Ru_2Rh_2H_2(CO)_{12}]$ which has been shown through solution NMR studies to undergo first hydrogen movement between the occupied and unoccupied Ru–Rh edges before exchange of the inequivalent hydrides associated with the Ru–Rh and Ru–Ru edges.[3]

Results and Discussion

1. Interstitial hydrides

The direct location of hydrogen in transition-metal hydride clusters relies heavily on neutron diffraction measurements. Claims for the presence of interstitial hydrides using other methods are fraught with difficulties as exemplified by the recent low-temperature neutron diffraction study of $[N(PPh_3)_2]_2[Os_{10}H_4(CO)_{24}]$ which shows the four hydrides to be on the surface of the metal framework in μ and μ_3 sites whereas earlier work suggested them to be all located in the interstitial sites.[8]

The only transition-metal carbonyl clusters which have been characterised by neutron diffraction and shown to have the hydride inside metal cavities, which are either octahedral or distorted octahedral, are shown in Table 1 together with the solution value of $\delta(^1H)$ for the hydride resonance. The chemical shift values in solution span a wide range and are essentially independent of cation and solvent for a given cluster. Tensor surface harmonic (TSH) theory has been used to account for the solution low-field chemical shifts of the Ru_6 and Co_6 clusters,[11] but we now show that there is a significant difference between solution- and solid-state values of $\delta(^1H)$ for $[Co_6H(CO)_{15}]^-$. Otherwise there is little variation in the values of the solution- and solid-state chemical shifts of the interstitial hydrides (Table 1).

For $[Co_6(H/D)(CO)_{15}]^-$ the ^{1}H MAS (magic angle spinning) NMR spectrum at room temperature (see Fig. 1) clearly shows a resonance at δ +1 for the interstitial hydride which disappears on deuteriation; the resonance at δ 0 in both Fig. 1(*a*) and 1(*b*) is due to Pr^{i}O(H/D), which was used for recrystallisation, and there is a broad resonance at δ 7 due to the cation. The resonances at δ 0 and 1 [Fig. 1(*a*)] exhibit only a small chemical shift anisotropy and comparison of their relative intensities suggests there is only a trace of residual Pr^{i}OH present as solvent of crystallisation which proved impossible to remove under high vacuum [10^{-3} mmHg (*ca.* 0.133 Pa) for 6 h]. The chemical shift value for the methyl group in neat Pr^{i}OH is δ 1.1 and the slight difference between $\delta(^1H)$ in solution and the

* Basis of the presentation given at Dalton Discussion No. 1, 3rd–5th January 1996, University of Southampton, UK.

Table 1 Solution- and solid-state NMR data for transition-metal carbonyl clusters containing interstitial hydrides

Cluster	Cation	Neutron diffraction ref.	Solution				Solid-state $\delta(^1H)$ at 298 K[a]
			Solvent	T/K	$\delta(^1H)$	Ref.	
$[Ru_6H(CO)_{18}]^-$	$AsPh_4^+$	4	CD_2Cl_2	298	16.4	4	18.5 ± 1[b]
	$N(PPh_3)_2^+$		CD_2Cl_2	313	16.4	9	15.5
	NMe_4^+		C_4D_8O	313	16.5	9	
$[Co_6H(CO)_{15}]^-$	$N(PPh_3)_2^+$	5	CH_2Cl_2	203	23.2	5	1
	PPh_4^+		CH_2Cl_2 or Me_2CO	173–223	23.5	5	
$[Ni_{12}H_2(CO)_{21}]^{2-}$	PPh_4^+	6	$(CD_3)_2CO$	313	−18.3	6	
	NEt_4^+		thf	298	−17.8[c]	This work	−19.9
$[Ni_{12}H(CO)_{21}]^{3-}$	PPh_4^+	6	CD_3CN	313	−24.4	6, 10	
	PPh_4^+		$(CD_3)_2CO$	313	−24.2		
	NEt_4^+						−26.8
	$NMe_3(CH_2Ph)^+$		$(CD_3)_2CO$	313	−24.2		

[a] Values of $\delta(^1H)$ are referenced to external $SiMe_4$. [b] Value for deuterium derivative; referenced to $SiMe_4$ *via* D_2O + 4.5 ppm. [c] $\delta(D)$ of the corresponding deuteride.

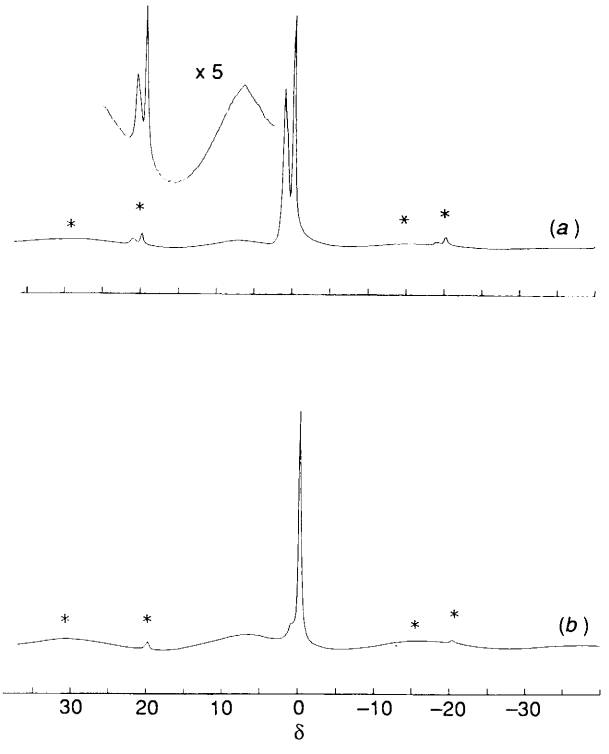

Fig. 1 Solid-state ^1H NMR spectra obtained on a Bruker MSL-200 spectrometer at room temperature for (*a*) $[N(PPh_3)_2][Co_6H(CO)_{15}]$ and (*b*) $[N(PPh_3)_2][Co_6D(CO)_{15}]$ at a spinning rate of 4.0 kHz. The asterisks indicate spinning side bands

Table 2 Metal–hydrogen distances and solid-state chemical shifts of carbonyl clusters containing interstitial hydrides

Cluster	Average M–H*/pm	$\delta(^1H)$
$[Ru_6H(CO)_{18}]^-$	203.7 (6)	+15.5
$[Co_6H(CO)_{15}]^-$	180.3 (4)	+1
	186.3 (2)	
$[Ni_{12}H_2(CO)_{21}]^{2-}$	184.5 (6)	−19.9
	200 (6)	
$[Ni_{12}H(CO)_{21}]^{3-}$	172 (3)	−26.8
	222 (3)	

* The value in parentheses indicates the number of M–H interactions.

solid state [Fig. 1(*a*) and 1(*b*)] is not unexpected.* The shift to higher field for $\delta(H)$ in the solid state on going from $[Ru_6H(CO)_{18}]^-$ to $[Co_6H(CO)_{15}]^-$ to $[Ni_{12}H_2(CO)_{21}]^{2-}$ corresponds to an increasing displacement of the interstitial hydride from the centre of the metal octahedral cavity as shown by neutron diffraction studies (see Table 2) and a decrease in symmetry of both the M_6 octahedron and the carbonyl distribution around the octahedral cavity. This reduction in symmetry results in a drastic change of the electronic state of the interstitial hydrogen, *i.e.* the lower the symmetry the lower is the paramagnetic contribution induced by the metal p and d electrons [or the more the shielding effect which gives a shift of $\delta(^1H)$ to high field]. Thus, these new data provide better evidence for the TSH theory being able to rationalise the variation in $\delta(^1H)$ of interstitial hydrides.

For the analogous interstitial deuteride derivatives, displacement of D from the centre of the octahedral cavity will result in an increased electric field gradient which contributes to an increased linewidth of the deuteride resonance. Thus, the half widths of the deuterium resonances at room temperature are *ca.* 1 and *ca.* 5 kHz for $[N(PPh_3)_2][Ru_6D(CO)_{18}]$ and $[N(PPh_3)_2][Co_6D(CO)_{15}]$ respectively (Fig. 2) and there is only a slight increase on lowering the temperature to 150 K; the large displacement of the deuterides towards the central Ni_6 layer prevents the observation of the D resonance in the dideuteride $[Ni_{12}D_2(CO)_{21}]^{2-}$.†

For $[Ni_{12}H(CO)_{21}]^{3-}$ a high-field ^1H resonance is observed both in solution and the solid state (Table 1). However, since only one ^{13}C resonance for each of the terminal and bridging COs on the outer $Ni_3(CO)_6$ layers can be observed both in solution (δ 228.1 and 196.8)[12] and the solid state (δ 228 and 199), we cannot be sure whether this is due to migration of H between the two octahedral metal cavities or because the H is static with the resonance of the inequivalent layers being coincident. Nevertheless, solution studies on the analogous derivative $[Ni_9Pt_3H(CO)_{21}]^{3-}$ suggest that migration of H between the interstitial octahedral sites occurs in solution.[13]

Nevertheless, irrespective of whether the hydride is static or migrating between equivalent sites on either side of the central Ni_3 triangle, the increased displacement of the hydride from the centre of the Ni_6 octahedron in $[Ni_{12}H(CO)_{21}]^{3-}$ is consistent with this cluster having the highest-field chemical shift (Table 2).

This work emphasises the importance of only relating spectroscopic and structural measurements on compounds *in the same phase* and is consistent with Chini's original proposal

* It proved impossible to observe solid-state interstitial ^1H or D resonances of $M[Co_6H(CO)_{15}]$ (M = K^+ or Cs^+) because of the cation being strongly solvated.

† The lack of change in H/D lineshape from 153 to 313 K suggests no change in migration of H/D within the octahedral/pseudo-octahedral cavities.

that the H atom in $[Co_6H(CO)_{15}]^-$ is involved in a rapid exchange *in solution* from the interstitial site to becoming associated with the carbonyl groups.[5,14] This explanation, which has for a long time been discounted, accounts for the anomalous low-field value of $\delta(^1H)$ in solution and the loss of the resonance when carrying out measurements both above 223 K and in deuteriated solvents.

2. $[Rh_{13}H_x(CO)_{24}]^{(5-x)-}$ (x = 2 or 3)

At room temperature, solution NMR measurements (^1H, ^{13}C and ^{103}Rh) showed that carbonyl migration occurred around the periphery of the Rh_{13} skeleton in both the di- and tri-hydride clusters together with interstitial migration of H which is probably concomitant with migration of CO.[7,15] In the case of $[Rh_{13}H_3(CO)_{24}]^{2-}$ it was possible to obtain low-temperature limiting spectra consistent with the solid-state structure and to establish the hydrogen-site occupancies; these were found to be on the square faces of the metal skeleton with preferential occupancy being faces with decreasing numbers of bridging carbonyls. It was also possible in this case to obtain the activation energy for hydrogen exchange ($\Delta G^{\ddagger}$ = 36.1 kJ mol^{-1}) but not the limiting low-temperature spectra of the dihydride derivative in order unambiguously to provide evidence for the hydrogen-site occupancy(s). As a result, we felt it to be worthwhile to investigate the behaviour of $[Rh_{13}H_x(CO)_{24}]^{(5-x)-}$ (x = 2 or 3) in the solid state and report their variable-temperature solid-state ^1H NMR spectra. As can be seen from Table 3, the solid-sate ^1H NMR chemical shifts at room temperature are very similar to the low-temperature limiting values obtained in solution. Furthermore, there is no evidence for migration of H in the solid state even on heating to 340 K. This is consistent with interstitial migration in solution being accompanied by a facile expansion of the internal Rh_3 faces of the Rh_{13} skeleton which becomes, in the solid state, of much higher energy because of intermolecular packing.

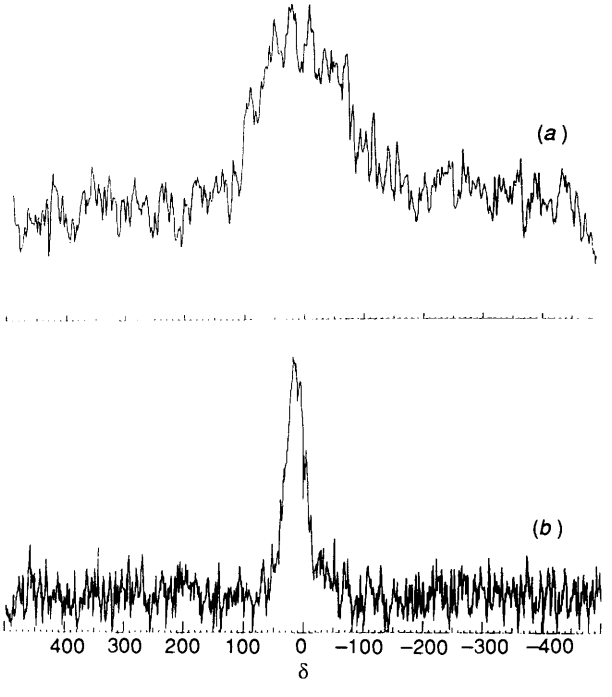

Fig. 2 Deuterium NMR spectra obtained on a Bruker MSL-200 spectrometer at room temperature using a static sample in a sealed 5 mm NMR tube: (*a*) $[N(PPh_3)_2][Co_6D(CO)_{15}]$, (*b*) $[N(PPh_3)_2][Ru_6D(CO)_{18}]$

3. $[Ru_2Rh_2H_2(CO)_{12}]$

The structure of $[Ru_2Rh_2H_2(CO)_{12}]$ is shown in Fig. 3; this was established by X-ray diffraction and the distinction of Ru from Rh through multinuclear NMR measurements.[3] This structure is related to the C_{3v} structures of $[M_4(CO)_{12}]$ (M = Co or Rh)[16] with H(1) bridging the Ru–Rh edge and H(2) the Ru–Ru edge. Both hydrides are almost coplanar with M_3 triangles; the dihedral angles between Rh(2)H(1)Ru(1)/Ru(1)-Rh(2)Rh(1) and Ru(3)H(2)Ru(1)/Ru(1)Ru(3)Rh(1) are 164 and 173° respectively.

Variable-temperature solution NMR measurements[3] are consistent with the instantaneous structure shown in Fig. 3 at low temperatures and at higher temperatures there is first the onset of exchange of H(1) between the occupied and unoccupied Rh–Ru edges followed by intra-exchange of H(1) with H(2).

The low-temperature solution ^1H NMR spectrum of $[Ru_2Rh_2H_2(CO)_{12}]$ showed two equally intense resonances at δ −19.2 and −21.3 with the former appearing as a doublet; this allowed the assignment of this resonance to H(1) (Fig. 3) as a result of coupling to Rh(2). The variable-temperature ^1H MAS NMR spectra of $[Ru_2Rh_2H_2(CO)_{12}]$ are presented in Fig. 4 and clearly show the presence of two high-field resonances (δ −19.5 and −21.6) with chemical shifts very similar to those observed at low temperature in solution; apart from an increase in the signal-to-noise ratio, there is little variation in the appearance of these resonances from 292 to 133 K and the lack of observation of Rh(2)–H(1) coupling, we feel, is due to lack of spectrometer resolution. The higher-field shift of H(2)

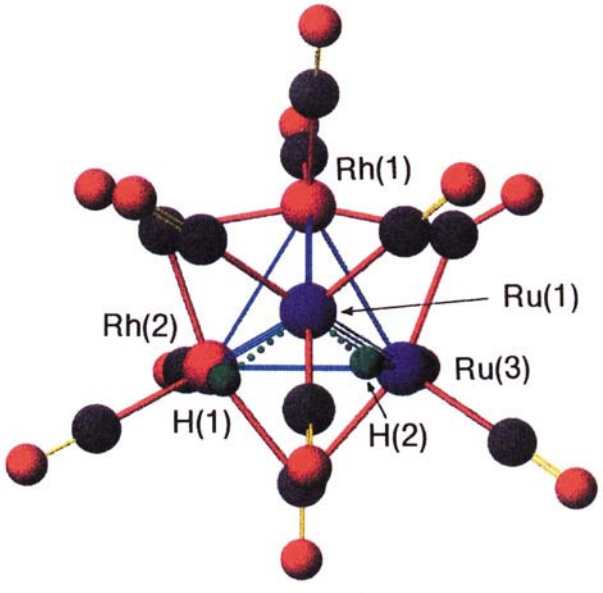

Fig. 3 Structure of $[Ru_2Rh_2H_2(CO)_{12}]$[3]

Table 3 Comparison of values for $\delta(H)$ in solution and the solid state for $[Rh_{13}H_x(CO)_{24}]^{(5-x)-}$ (x = 2 or 3)

	Solution		Solid state	
Cluster	T/K	$\delta(^1H)$*	T/K	$\delta(^1H)$*
$[Rh_{13}H_2(CO)_{24}]^{3-}$	178	−27.0(1), −27.9(1)	298–340	−26.0(1), −27.8(1)
$[Rh_{13}H_3(CO)_{24}]^{2-}$	183	−28.2(1), −31.1(2)	298–340	−28.1(1), −31.6(2)

* Figures in parentheses refer to relative intensities.

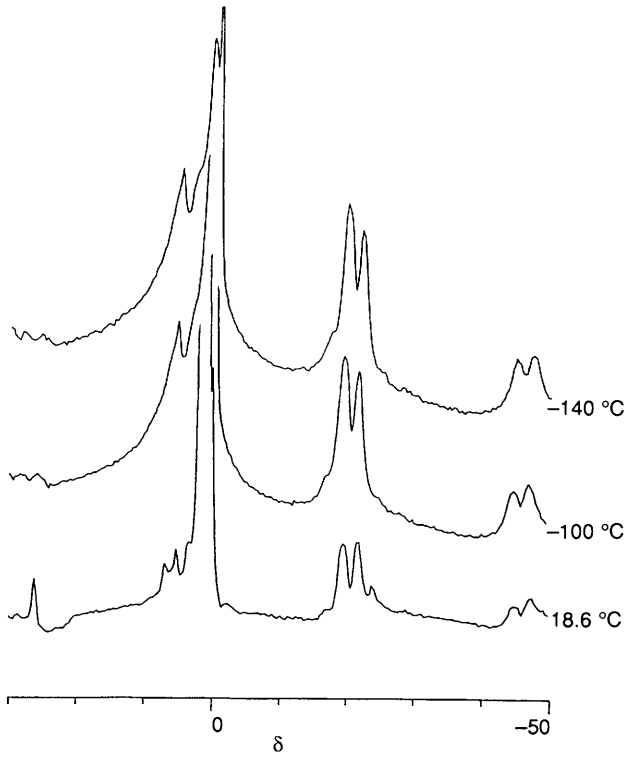

Fig. 4 Variable-temperature ^{1}H MAS NMR spectra of $[Ru_2Rh_2H_2(CO)_{12}]$ at a spinning rate of 5.0 kHz

compared to H(1) is in keeping with H(2) being closer {*d*[Ru(1)–H(2)] 1.452, *d*[Ru(3)–H(2)] 1.595 Å} to the Ru–Ru edge (more shielded) than H(1) is to the Rh–Ru edge {less shielded, *d*[Ru(1)–H(1)], 1.664, *d*[Rh(2)–H(1)] 1.763 Å}; these variations in *d*(M–H) are consistent with the expected preferential hydrogen-site occupancy of Ru–Ru > Ru–Rh > Rh–Rh edge which has recently been confirmed for $[Ru_2Rh_2H(CO)_{12}]^-$.[17] Fig. 4 also clearly shows the presence of a resonance near δ 0 which we attribute to a small amount of residual solvent (acetone) of crystallisation which could not be removed even under high vacuum.

In order further to investigate the motion in the solid state of H(1) and H(2) in $[Ru_2Rh_2H_2(CO)_{12}]$, we measured the temperature dependence of the proton spin–lattice relaxation time by using the inversion-recovery method at 200 MHz using MAS (Fig. 5) and by using a pulsed wide-line spectrometer at 40.4 MHz. Results from both measurements are shown in Fig. 6 which clearly show that: (*a*) T_1 of the hydrides is much longer than T_1 for the solvent and these values can only be differentiated by MAS measurements; (*b*) the T_1 value obtained using the pulsed wide-line spectrometer is dominated by the solvent; and (*c*) the T_1 temperature dependence for the residual solvent indicates a correlation time for molecular motion in the range $\omega_0\tau_c \ll 1$ (ω_0 = Larmor frequency, τ_c = correlation time) with an estimated activation energy E_a of *ca.* 5 kJ mol^{-1}, whereas there is a very weak temperature dependence of T_1 for the hydrides with E_a *ca.* 1 kJ mol^{-1}.

The distance between H(1) and H(2) is 2.04 Å and this leads to dipole–dipole interaction being the main relaxation mechanism for the hydride ligands in $[Ru_2Rh_2H_2(CO)_{12}]$. A small change in the proton–proton vector could be responsible for the observed data and from equations (1) [γ = gyromagnetic ratio, r_{H-H} = distance between H(1) and H(2)] and (2), if θ is 16°,* the minimum T_1 value is *ca.* 3.3 s at $\omega_0\tau_C = 0.616$. From

* If H(1) moves from being coplanar with the Ru(1)Rh(2)Rh(1) triangle to become coplanar with the Ru(1)Rh(2)Ru(3) triangle, then the change in H–H vector, θ, is 16° and the H(1)–H(2) separation changes from 2.04 to 2.345 Å.

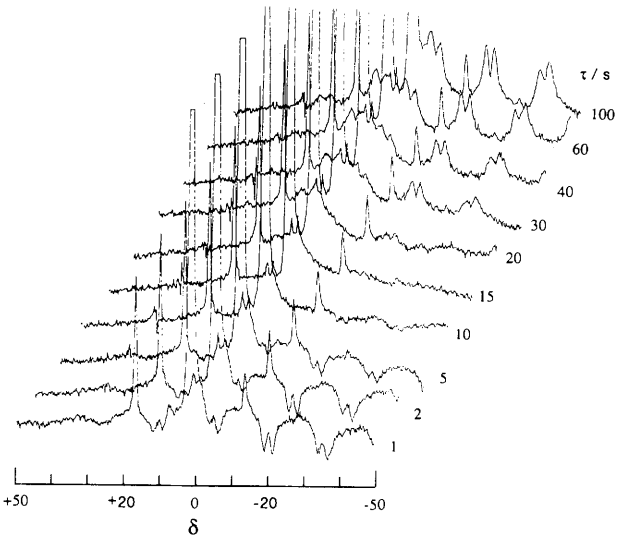

Fig. 5 Delay time (τ) dependence of ^{1}H MAS NMR spectra for $[Ru_2Rh_2H_2(CO)_{12}]$ from inversion-recovery measurements at 200 MHz

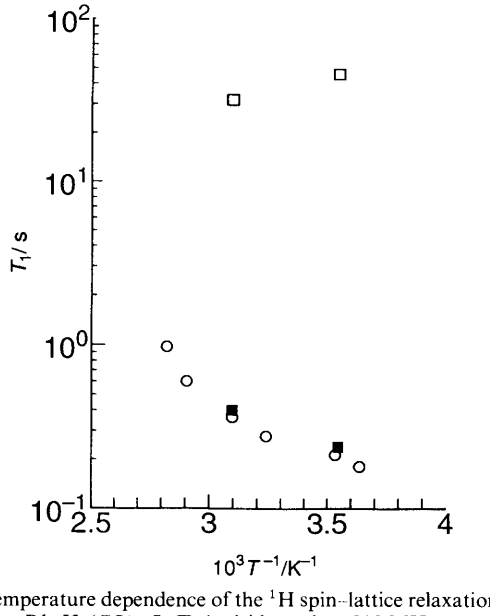

Fig. 6 Temperature dependence of the ^{1}H spin–lattice relaxation time in solid $[Ru_2Rh_2H_2(CO)_{12}]$: □, hydride peak at 200 MHz; ○, solvent peak at 200 MHz; ■, wide-line measurements at 40.4 MHz

$$T_1^{-1} = \frac{9}{20}\sin^2\theta\,\frac{\gamma^4\hbar^2}{r_{H-H}^6}\,B(\tau_c) \qquad (1)$$

$$B(\tau_c) = \frac{\tau_c}{1+\omega_0^2\tau_c^2} + \frac{4\tau_c}{1+4\omega_0^2\tau_c^2} \qquad (2)$$

the observed T_1 values in Fig. 6, we could not expect the appearance of such a short T_1 minimum below 400 K, suggesting θ < 16° and a slow hydrogen-motion in the range $\omega_0\tau_C \gg 1$. Such small displacements of the H(1)–H(2) vector would result from either one or both hydrides oscillating to equalise *d*(M–H) while remaining coplanar with the M_3 triangles as found by X-ray analysis, or through oscillation about the metal edge to become coplanar with the adjacent M_3 triangle.* The above explanation eliminates any possibility of the hydrogen migration in the solid state resembling that found in solution. For the rearrangement found in solution to occur in the solid state there would have to be a gross rearrangement of the distorted carbonyl icosahedron associated with each

molecule since incorporation of hydrides results in a significant expansion of the carbonyl icosahedron in adjacent areas (see Fig. 7), and the two molecules in the unit cell (see Fig. 8) are already efficiently close-packed to minimise these distortions.

This explanation differs from that recently proposed for $[Ru_4H_4(CO)_{12}]$.[18] In that case, the large T_1 temperature dependence gave a value of $E_a = 67.2$ kJ mol^{-1} which, together with other data, was interpreted as being due to either (*a*) rotation of the Ru_4, together with the edge-bridging hydrides, about the C_2 axis, or (*b*) a concerted movement of the four hydrides over the occupied/unoccupied edges of the Ru_4 tetrahedron. For $[Ru_4H_4(CO)_{12}]$ the T_1 temperature-dependent measurements were obtained using a pulsed wide-line spectrometer. Since this sample also contained solvent of crystallisation, it is questionable as to whether the reported T_1 temperature dependence relates to the hydride as we have shown that similar measurements on $[Ru_2Rh_2H_2(CO)_{12}]$, which also contains solvent of crystallisation, are dominated by solvent (see Fig. 6).

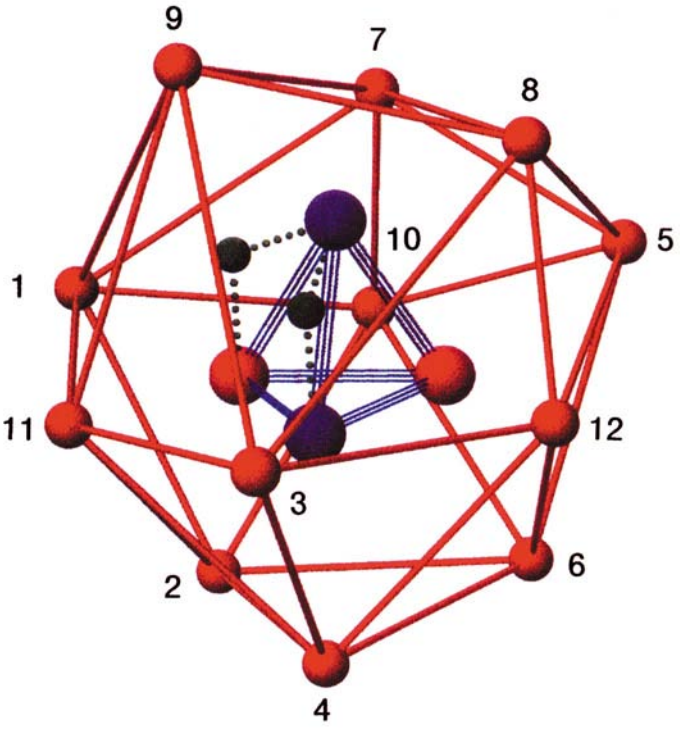

Fig. 7 Schematic representation of the distorted oxygen icosahedron incorporating the $Ru_2Rh_2H_2$ core for $[Ru_2Rh_2H_2(CO)_{12}]$. The shortest and longest O···O contacts are O(7)···O(10) and O(3)···O(8), 3.336 and 5.747 Å respectively

Experimental

A Bruker MSL-200 spectrometer was used to obtain ^{1}H MAS and D NMR spectra and ^{1}H T_1 values using MAS. The ^{1}H MAS NMR spectra at low temperature were measured on a Chemagnetic CMX 200H spectrometer operating at 200 MHz. The ^{1}H spin–lattice relaxation times, T_1, of static samples were measured on a JEOL FSE60SS pulsed spectrometer operating at 40.4 MHz.

The compounds $[Ru_6H(CO)_{18}]^-$,[9] $[Co_6H(CO)_{15}]^-$,[5] $[Ni_{12}H_x(CO)_{21}]^{(4-x)-}$ ($x = 1$ or 2),[10,12] $[Rh_{13}H_x(CO)_{24}]^{(5-x)-}$ ($x = 2$ or 3)[7] with the desired cation and $[Ru_2Rh_2H_2(CO)_{12}]$[3] were prepared according to published procedures. Deuterium-enriched samples were obtained easiest by direct exchange through stirring a tetrahydrofuran (thf) or acetone solution containing the hydride derivative for 4 h under an atmosphere of deuterium, freezing the solution, evacuating the gas and stirring again under deuterium, followed by recrystallisation.

Acknowledgements

We thank the EPSRC, EC (contract No. CHRX-CT93-0277) and the Japanese Society for the Promotion of Science for financial support and the Royal Society and British Council for travel funds. We thank Miss T. Akai for the low-temperature ^{1}H MAS NMR measurements.

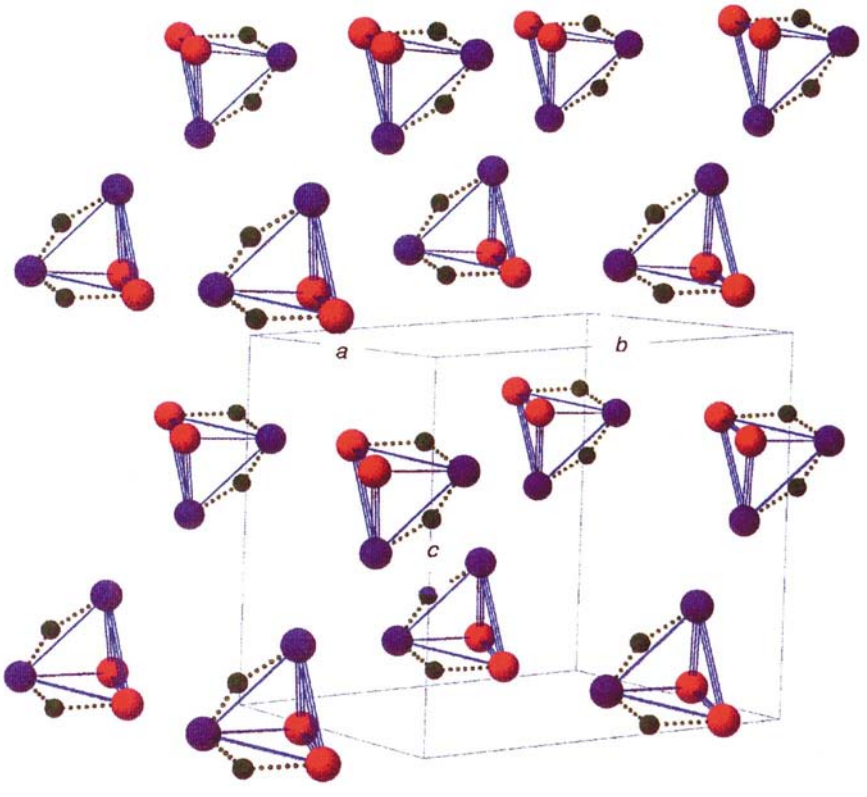

Fig. 8 The crystal packing of $[Ru_2Rh_2H_2(CO)_{12}]$ as represented by the $Ru_2Rh_2H_2$ core. For colour code see Fig. 3

References

1 B. T. Heaton, L. Strona, S. Martinengo, D. Strumolo, R. J. Goodfellow and I. H. Sadler, *J. Chem. Soc., Dalton Trans.*, 1982, 1499.

2 S. Bordoni, B. T. Heaton, C. Seregni, L. Strona, R. J. Goodfellow, M. B. Hursthouse, M. Thornton-Pett and S. Martinengo, *J. Chem. Soc., Dalton Trans.*, 1988, 2103.

3 J. Pursiainen, T. A. Pakkanen, B. T. Heaton, C. Seregni and R. J. Goodfellow, *J. Chem. Soc., Dalton Trans.*, 1986, 681.

4 P. F. Jackson, B. F. G. Johnson, J. Lewis, P. R. Raithby, M. McPartlin, W. J. H. Nelson, K. D. Rouse, J. Allibon and S. A. Mason, *J. Chem. Soc., Chem. Commun.*, 1980, 295.

5 D. W. Hart, R. G. Teller, C.-Y. Wei, R. Bau, G. Longoni, S. Campanella, P. Chini and T. F. Koetzle, *J. Am. Chem. Soc.*, 1981, **103**, 1458.

6 R. W. Broach, L. F. Dahl, G. Longoni, P. Chini, A. J. Schulz and J. M. Williams, *Adv. Chem. Ser.*, 1978, **167**, 93.

7 C. Allevi, B. T. Heaton, C. Seregni, L. Strona, R. J. Goodfellow, P. Chini and S. Martinengo, *J. Chem. Soc., Dalton Trans.*, 1986, 1375.

8 A. Bashall, L. H. Gade, J. Lewis, B. F. G. Johnson, G. J. McIntyre and M. McPartlin, *Angew. Chem.*, 1991, **103**, 1186.

9 C. R. Eady, P. F. Jackson, B. F. G. Johnson, J. Lewis, M. Malatesta, M. McPartlin and W. J. H. Nelson, *J. Chem. Soc., Dalton Trans.*, 1980, 383.

10 A. Cerrioti, P. Chini, R. Della Pergola and G. Longoni, *Inorg. Chem.*, 1983, **221**, 1595.

11 M. J. Duer and D. J. Wales, *Polyhedron*, 1991, **10**, 1749.

12 G. Longoni, P. Chini and B. T. Heaton, *J. Chem. Soc., Dalton Trans.*, 1980, 1537.

13 A. Ceriotti, F. Demartin, B. T. Heaton, G. Longoni, M. Manassero, G. Piro, G. Piva and M. Sansoni, *J. Organomet. Chem.*, 1986, **301**, C5.

14 P. Chini, G. Longoni, S. Martinengo and A. Ceriotti, *Adv. Chem. Ser.*, 1978, **167**, 1.

15 S. Martinengo, B. T. Heaton, R. J. Goodfellow and P. Chini, *J. Chem. Soc., Chem. Commun.*, 1977, 309.

16 C. H. Wei, *Inorg. Chem.*, 1969, **8**, 2384; F. H. Carré, F. Cotton and B. A. Frenz, *Inorg. Chem.*, 1976, **15**, 380.

17 A. Fumagalli, M. C. Malatesta, M. Bianchi, P. Carra, G. Ciani, M. Moret and A. Sironi, ESF Workshop, Bimetallic Effects in Chemistry, Parma, April 1995.

18 S. Aime, R. Gobetto, A. Orlandi, C. J. Groombridge, G. E. Hawkes, M. D. Mantle and K. D. Sales, *Organometallics*, 1994, **13**, 2375.

Received 25*th July* 1995; *Paper* 5/06040K